ARCHITECTURAL RESEARCH, Vol.25, No.1(March 2023). pp.1-9 pISSN 1229-6163 eISSN 2383-5575

Seismic Retrofit Assessment of Different Bracing Systems

Sudipta Chakraborty[1], Md. Rajibul Islam[1], Dookie Kim[2] and Jeong Young Lee[1]

[1] Graduates, Department of Civil and Environmental Engineering, Crash & Quake Research Center, Smart Natural Space Research Center, Kongju National University, Cheonan, Korea

[2] Professor, Department of Civil and Environmental Engineering, Crash & Quake Research Center, Smart Natural Space Research Center, Kongju National University, Cheonan, Korea

https://doi.org/10.5659/AIKAR.2023.25.1.1

Abstract Structural ageing influences the structural performance in a negative way by reducing the seismic resilience of the structure which makes it a major concern around the world. Retrofitting is considered to be a pragmatic and feasible solution to address this issue. Numerous retrofitting techniques are devised by researchers over the years. The viability of using steel bracings as retrofitting component is evaluated on a G+30 storied building model designed according to ACI318-14 and ASCE 7-16. Four different types of steel bracing arrangements (V, Inverted V/ Chevron, Cross/ X, Diagonal) are assessed in the model developed in commercial nu-merical analysis software while considering both material and geometric nonlinearities. Reducing displacement and cost in the structures indicates that the design is safe and economical. Therefore, the purpose of this article is to find the best bracing system that causes minimum displacement, which indicates maximum lateral stiffness. To evaluate the seismic vulnerability of each system, incremental dynamic analysis was conducted to develop fragility curves, followed by the formation of collapse margin ratio (CMR) as stipulated in FEMA P695 and finally, a cost estimation was made for each system. The outcomes revealed that the effects of ge-ometric nonlinearity tend to evoke hazardous consequences if not considered in the structural design. Probabilistic seismic and economic probes indicated the superior performance of V braced frame system and its competency to be a germane technique for retrofitting.

Keywords: Retrofitting method, Steel bracing, Nonlinear dynamic analysis, Seismic fragility analysis, Collapse margin ratio

1. INTRODUCTION

As the global population is growing rapidly, ensuring a safe accommodation facility for this verbiage population has become a burning question around the world and high-rise multistoried buildings are considered to be the perfect supplants to solve this universal issue. To construct high-rise buildings, concrete is the most preferred material throughout the twentieth century due to its cheap cost and great structural strength (Lakshmanan 2006).

Corresponding Author : Dookie Kim

Department of Civil and Environmental Engineering, Crash & Quake Research Center, Smart Natural Space Research Center, Kongju National University, 1223-24 Cheonan-daero, Seobuk-gu, Cheonan, Chungcheongnam-do, Korea
e-mail : kim2kie@kongju.ac.kr

This research was supported by UNDERGROUND CITY OF THE FUTURE program funded by the Ministry of Science and ICT.

However, the construction of high-rise building is quite complex as their structural design necessitate the consideration of various parameters required to satisfy the structural safety and serviceability considerations (Avinash & Pandian 2017). P-Delta (P-Δ) effect is one such important factor that significantly affects the stability and ductility of the structure. P-delta effect, also known as the second-order effect or Geometric nonlinearity, originates from a destabilizing moment when the structure is under significant vertical and lateral load at the same time. Lateral deformations induced by wind and seismic events tend to develop P-Delta effects which bring lethal consequences, especially for tall structures (Kumar 2019). The magnitude of P-Delta effect is related to the stiffness and slenderness of both the whole structure and individual structural constituents. Numerous studies have been conducted to analyze P-Delta effects. Avinash & Pandian (2017) utilized a 42 storied tabular building model with nine different plan dimensions in ETABS software to observe P-Δ effects in terms of bending moment and lateral deflection. They considered aspect ratio, height to least lateral plan dimension and the lateral stiffness as the governing parameters to quantify P-Δ effects. Their investigation revealed that P-Δ effects tend to ascend with decreasing lateral stiffness. Islam et al. (2022) and Chakraborty et al. (2022) examined the structural behavior of buildings under extreme lateral loadings using ETABS software while Cheng et al. (2022) compared the effects of P-Δ on the nonlinear seismic response of steel moment-resisting frame structures (MRFs) under near-fault and far-fault ground motions. Three steel building models- 3, 9 and 20 storied were utilized while 50 sets of ground motions were employed to quantify P-Δ effects in terms of peak inter-story drift ratio (PIDR) demands. They ended their study with the conclusion that P-Δ effects should be considered with more emphasis during the structural design and analysis phase as it becomes significant with the increasing intensity of earthquake. Abbas & Hassoni (2018) conducted both static and dynamic analysis on different steel buildings having varying heights and different bracing arrangements in ETABS software while integrating P-Δ effects in order to perceive its effects on the seismic response of high-rise structures. They explored that inclusion of P-Δ effects tend to remarkably increase the displacement and drift in buildings larger than 20 stories. From their study, Abdulkareem & Abbas (2020) came up with the decision that addition of P-Δ effects diminishes the pseudo acceleration of the building though the inter-story drift tends to increase. Kumar. (2019) analyzed the effects of geometric nonlinearity (P-Δ) on the seismic performance of multistoried RC structures and results exhibited that overlooking P- Δ effects may lead to the collapse of buildings under earthquake events. Khan et al. (2019) and Chakrawarty (2022) developed three varying storied RC framed buildings and performed nonlinear static analysis with P-Δ effects to evaluate the effects induced by geometric nonlinearity. The outcomes of the analysis divulged that modeling of the buildings greater than 75m should incorporate the geometric nonlinearity (P-Δ) effects.

As P-Delta effect is most prominent when subjected to seismic events and earthquake events are sporadic yet disastrous and life-threatening incidents, incorporation of apropos earthquake resistant systems in buildings is an indispensable criterion for confirming structural safety. In addition, structural lifetime is another important factor in the structural design. Every structure has a certain serviceability period after which some modifications in several structural features might be required for ensuring adequate performance under seismic events. This re-strengthening of existing structures is termed as retrofitting technique which is proven to be quite effective in providing sufficient seismic resistance to the aged structures. During the past decade, numerous studies has been conducted regarding the novel methods of retrofitting of existing structures, some integrating fragility curves as they are considered the most precise probabilistic damage indicator under various damage states. Islam et al. (2023) performed fragility analysis to investigate the seismic retrofitting performance of combined earthquake resistant systems while Navya & Agarwal (2016) executed seismic evaluation on a building retrofitted with steel bracings utilizing two different code provisions along with fragility analysis for both models. Carofilis Gallo et al. (2022) conducted a multi-criteria decision-making assessment on the seismic resilience of several retrofitted school buildings in Italy by critically analyzing existing evaluation frameworks to observe the impact of resilience on the retrofitting strategies. Incorporation of steel bracings is one of the most popular retrofitting techniques around the world because of its easy installation and great resilience. Researchers have also confirmed its ability to provide better seismic resilience. Goudar & Talasadar (2017) executed a buckling analysis of RC buildings having several types of bracings while considering P-Δ effects. The findings from the results clearly illustrated the competency of bracing systems in resisting the stiffness as well as the buckling of the structure. Islam et al. (2022) investigated the influence of nonlinearities induced by structural components by analyzing three G+10 building models with shear wall and steel bracings and found steel bracings to be quite efficacious in resisting nonlinear seismic responses. Garg & Sharma (2020); Viji et al. (2022); Eskandari et al. (2017) and Verma & Singi (2022) also found steel bracings to be a better performer under seismic conditions. The aims and objective of this study were to investigate:

(i) the effects of geometric nonlinearity (P-Delta) on the seismic responses of the structure

(ii) the seismic vulnerability of structures equipped with different bracings as earthquake resistant systems

(iii) the retrofitting potential of bracings from the seismic performance.

2. METHODOLOGY

In this article, the seismic behavior of a G+30 storied building retrofitted with four different types of steel bracings (Inverted V/ Chevron, V, Diagonal, Cross/X) is investigated to observe their retrofitting potential. The shape of the building is chosen as square because this is one of the most common shapes selected for majority of the buildings. All the building models are designed as per the ACI 318-14 and ASCE 7-16 code provisions and developed in ETABS (v.18) software. Details of building models are presented in Table-1 and Table-2 respectively. The properties of steel bracing used in this study are illustrated in Table-3. Five sets of strong ground motion data obtained from Pacific Earthquake Engineering Research Center (PEER) database that were spectrally matched to the selected zone were used to perform nonlinear time-history analysis and their details are shown in Table-4. To incorporate the effects of nonlinearity, both material (Plastic hinge) and geometric (P-Δ and large displacement) nonlinearities were considered. Material nonlinearities are introduced by assigning P-M2-M3 interacting isotropic hinges at both ends of beams and columns, which turns the connection between beams and columns into semi-rigid. The moment-rotation curve for plastic hinge is presented in Figure-2(h). P-Δ and large displacement module in ETABS is utilized to take the geometric nonlinear effects into account. Slabs are defined as rigid diaphragms while they are modeled using shell elements. In order to develop fragility curves and evaluate the damage states as per the performance levels specified by Xue et al. (2008), incremental dynamic analysis (IDA) was performed to create IDA curves for all the models. Then from the collapse fragility curves, collapse margin ratio was calculated as per FEMA P695, followed by the cost analysis of different braced systems. The whole workflow is graphically represented in Figure-1. Figure-2 illustrates the 3D representation of all the analyzed models.

Table 1. Parameters used for building models

Story Number	30 (G+30 Building)
Concrete Grade	M45(Column and Shear wall), M40 (Slab and Beam)
Steel Grade	S235
Beam Dimension	500mm*600mm
Column Dimension	1000mm*1000mm
Slab Thickness	150mm
Shear wall (SW) Thickness	250mm
Story Height	3.2m
Dead Load	1kN/m2
Live Load	5kN/m2
Density of Concrete	25kN/m3
Considered Load Types	Dead, Live, Earthquake, Wind
Seismic Zone	3
Site Class	SD
Importance factor (I)	1
Response Reduction Factor, R	6
System Over strength Factor, Ω	2.5
Deflection Amplification, Cd	5
Damping Ratio	5%
Basic Wind Speed	100 mph
Seismic design category (as per FEMA)	C
RCC Design Code	ACI 318-14
Earthquake Design Code	ASCE 7-16

Table 2. Details of building models developed in ETABS

Model-1	BF	Bare frame (no steel bracing)
Model-2	DB	Frame with diagonal bracing
Model-3	VB	Frame with V bracing
Model-4	CB	Frame with inverted V/ Chevron bracing
Model-5	XB	Frame with cross/ X bracing

Table 3. Details of selected steel bracing

Cross-section	UPE 220
Type	Concentric
Shape	U type
Cross-sectional area (cm2)	38.5
Nominal weight/1m (kg/m)	26.6

Table 4. Details of selected ground motions

Seismic event	Year	Magnitude	PGA (g)
Kobe, Japan	1995	6.9	0.233
Loma, USA	1989	6.9	0.26
EL Centro, USA	1940	6.9	0.348
Chi Chi, Japan	1999	7.7	0.42
Nahanni, Canada	1985	6.9	0.54

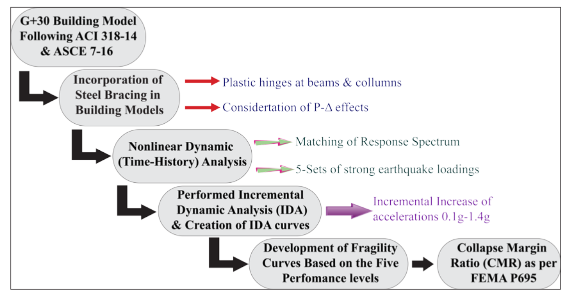

Figure 1. Schematic flow diagram of the analysis methodology.

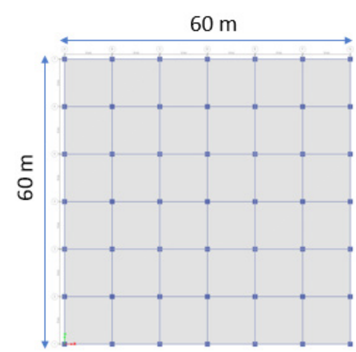

(a) Plan view of all building models

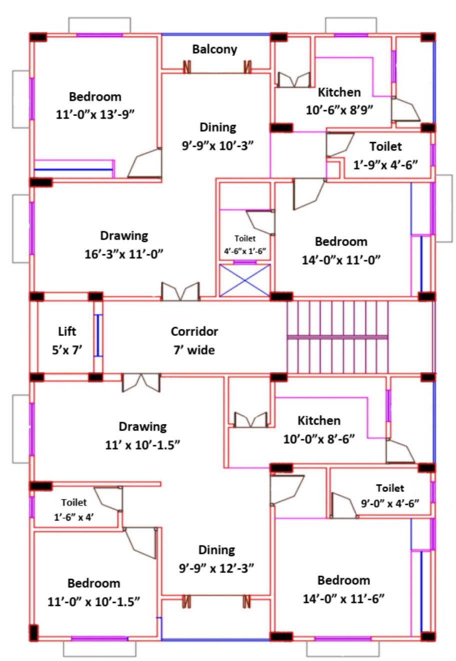

(b) Typical floor plan of all building models

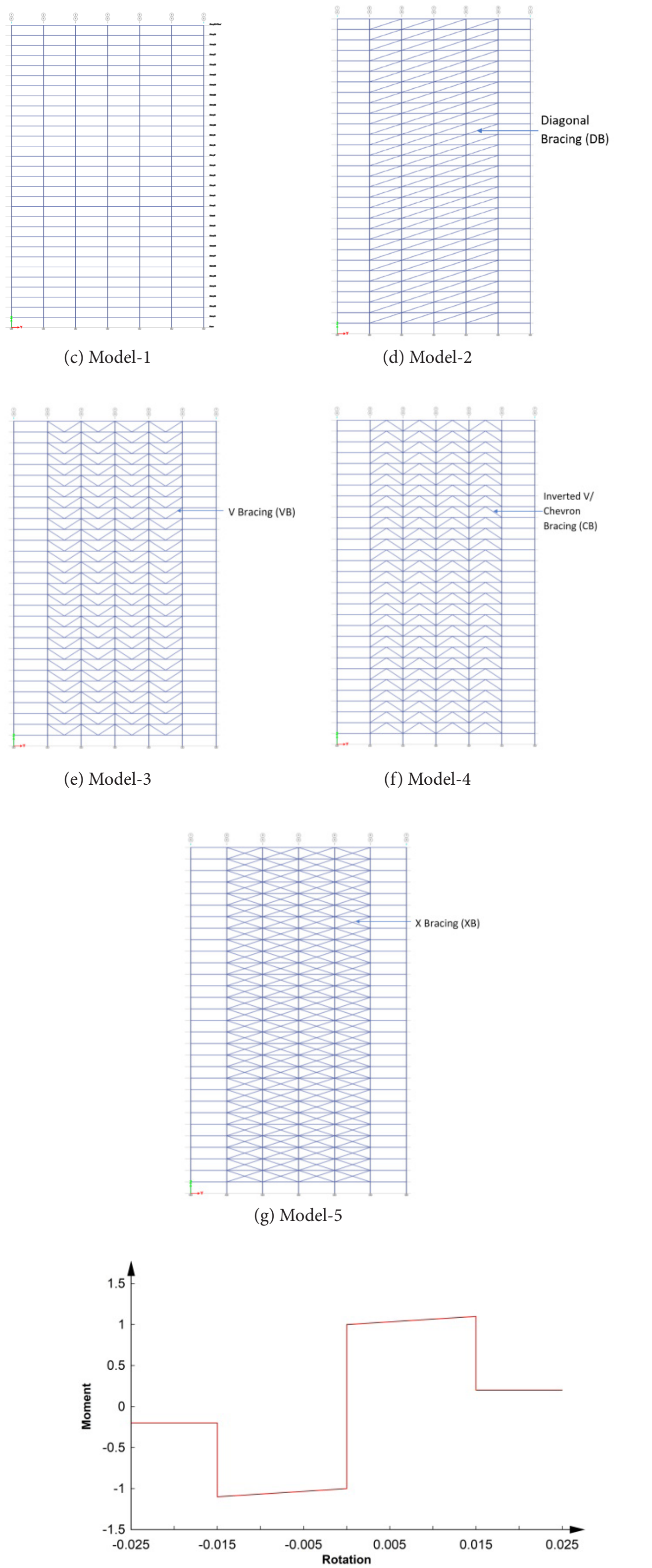

(c) Model-1 (d) Model-2

(e) Model-3 (f) Model-4

(g) Model-5

(h) Moment-Rotation curve of plastic hinge

Figure 2. Plan view, Floor plan, Elevation of all models and Moment- Rotation relationship of plastic hinges

3. ANALYSIS AND RESULTS

Five structural models were developed and numerically analyzed in commercial building analysis software ETABS (v.18) to investigate the retrofitting potential of different bracing systems. As per the provisions of ASCE 7-16, five sets of ground motions were selected to perform nonlinear time-history analysis (NLTHA) to observe the seismic responses. All the ground motions were spectrally matched to the target spectrum of the selected zone as depicted in Figure-3. The results derived from the analysis are rigorously discussed in the following parts.

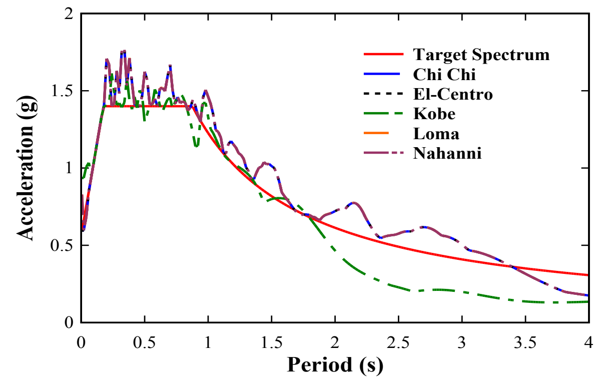

Figure 3. Spectrally matched ground motions

(1) Displacement

The lateral displacement of a particular story with respect to the base, when subjected to wind and earthquake loadings, is termed story displacement. Figure-4 illustrates the displacement of all the models under different earthquakes.

From the comparison of the displacement curves obtained from each ground motion, it is clear that the effect of geometric nonlinearity on the story displacement is quite large due to the large amount of lateral loading induced by the seismic tremor that produces an additional moment. With the increase in height, displacement tends to ascend linearly to a higher magnitude in all the building models. While analyzing the results of the analyses with and without the consideration of P-Δ effects, it becomes evident that Model-3 (V braced frame) manifests the best resistance against the lateral loads, followed by Model-4 (Inverted V/ Chevron braced frame).

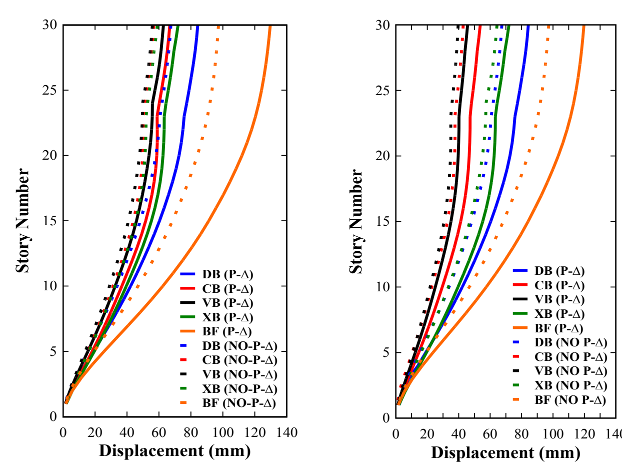

(a) Kobe earthquake (b) Loma earthquake

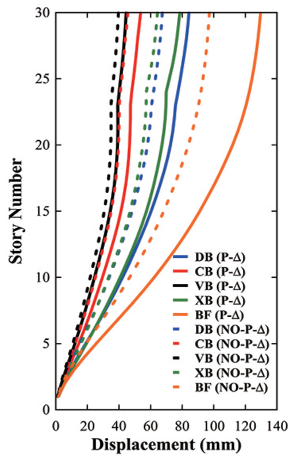

(c) Nahanni earthquake

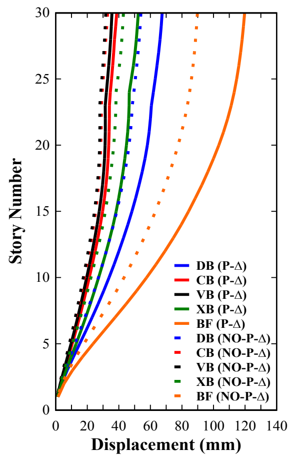

(d) Chi Chi earthquake

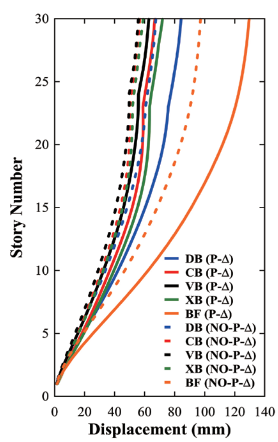

(e) El-Centro earthquake

Figure 4. Story displacement of all models.

(2) Interstory drift ratio

The ratio between the relative displacements of a particular story to the height of that story is known as interstory drift ratio (IDR).

Drift ratio is considered as an important engineering demand parameter (EDP) which can be used for forecasting the probability of structural damage. Figure-5 demonstrates the interstory drift ratio of all the models under different earthquakes. From the observation, it can be said that IDR values for all structures followed the same pattern, values being ascended linearly from the bottom up to the 8th story and plummeting sharply all the way to the top story. This huge IDR from the 3rd to the 8th story occurred because of the formation of plastic hinges at these levels which triggered the drift values of these stories. As displacement and drift are proportional to each other, similar trend is also observed in case of IDR as Model-3 (V-framed structure) again outshines other models in terms of seismic resilience. Considering both displacement and IDR values of all models, the hierarchical order of best performing system is as follows: Model-3>Model-4>Model-5>Model-2>Model-1.

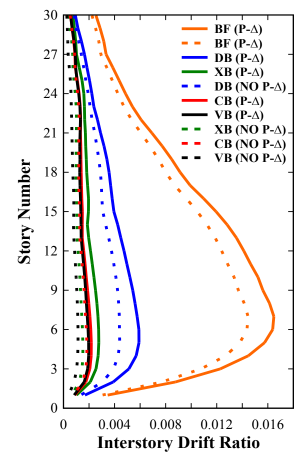

(a) Kobe earthquake

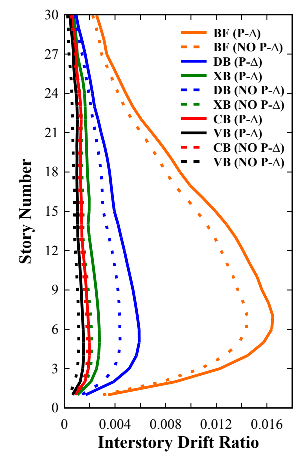

(b) Loma earthquake

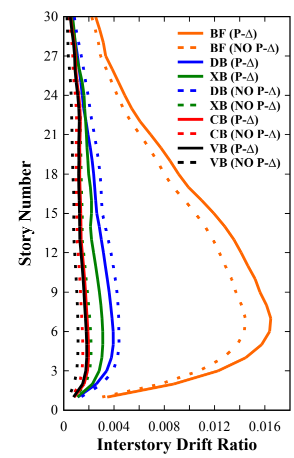

(c) Nahanni earthquake

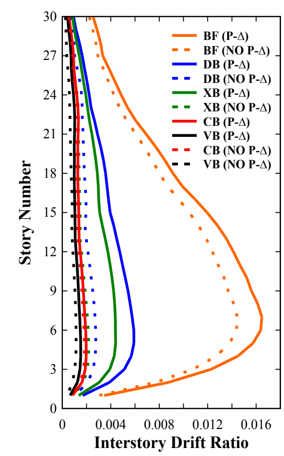

(d) Chi Chi earthquake

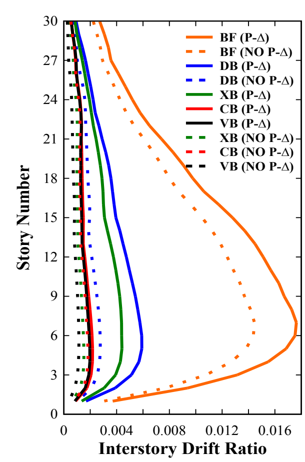

(e) El-Centro earthquake

Figure 5. IDR for all models.

(3) Story shear

The reaction that each column of the building, has on each floor of the building supposing the column is simply supported is labeled as story shear, the lateral force induced by wind and seismic actions on a story. Generally, shear is found minimum at the top and maximum at the bottom of the building. Same pattern was followed for each earthquake loads both for with and without P-Δ effect. Due to page limitations all the shear force curves for all the earthquake loads are not presented here in this manuscript, as the representative story shear curves from Kobe and El-Centro earthquakes are depicted in the Figure 6. For all the earthquakes maximum shear forces were found while analyses were performed considering P-Δ effect as described in the Table 5. Story shear values from the plots clearly indicate the same trend as observed previously for displacement and drift values. Maximum shear values were found at base for all the cases. Maximum shear forces were observed for BF building systems and minimum for VB structural systems. Five earthquakes, El-Centro, Kobe, Loma, Chi Chi and Nahanni are presented as E, K, L, C and N, respectively; as described in the Table 5.

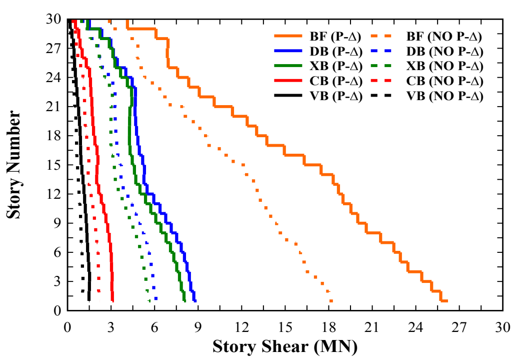

(a) Kobe earthquake

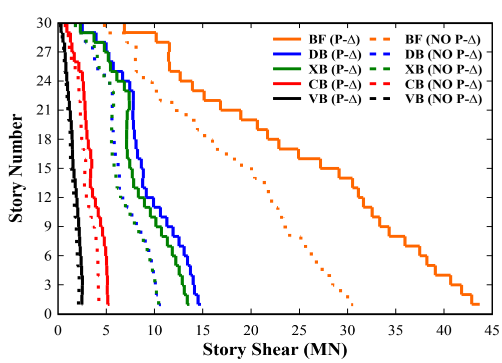

(b) El-Centro earthquake

Figure 6. Story shear of all models

Table 5. Maximum Shear force values

EQs	P-Δ Effect	BF	DB	XB	CB	VB
E	P-Δ	43.7	14.8	13.6	5.3	2.5
	NP-Δ	30.5	10.6	10.6	4.3	2.1
K	P-Δ	26.2	8.8	8.1	3.1	1.5
	NP-Δ	18.3	6.2	5.7	2.2	1.05
L	P-Δ	32.1	22.6	21.3	20.4	19.2
	NP-Δ	30.5	18.3	17.6	16.7	15.3
C	P-Δ	29.2	20.1	17.8	14.8	12.3
	NP-Δ	20.5	14.4	13.9	12.1	10.6
N	P-Δ	20.1	12.2	10.5	10.3	9.1
	NP-Δ	14.1	8.8	8.5	8.1	7.8

*All the units are in MN, NPΔ- No P-Δ

(4) Bending Moment

The trends of bending moments exhibited the similar phenomena as like the shear forces. Maximum magnitudes of moments found during the analysis considering P-Δ effect. Figure 7 represents the moment profile for the Kobe earthquake both for X and Y axis with and without considering P-Δ effect. The similar trends were also observed for rest of the four earthquake loads, due to page limitations rest of the curves is skipped. Significant moment was developed in the BF systems and less amount moment was generated for the VB building systems. Table 6 presents the magnitudes of momentum for the all the earthquake loads considering with and without P-Δ effect. Maximum momentum was obtained at base. Five earthquakes, El-Centro, Kobe, Loma, Chi Chi and Nahanni are presented as E, K, L, C and N, respectively; as described in the Table 6.

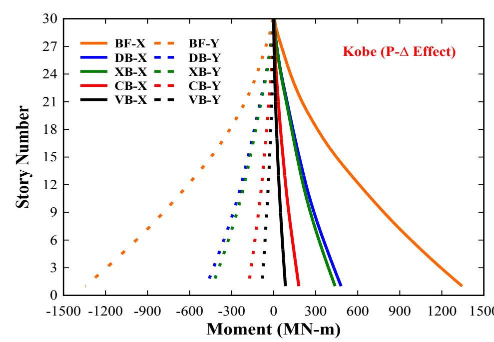

(a) Moment considering P-Δ effect

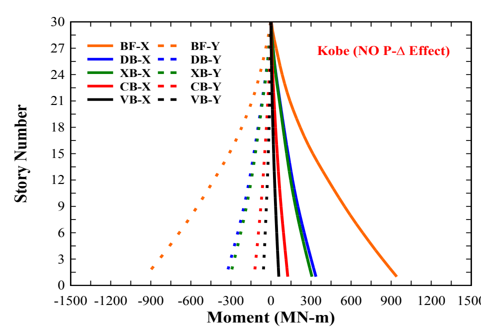

(b) Moment without considering P-Δ effect

Figure 7. Bending moment considering with and without P-Δ effect.

Table 6. Developed maximum moment for the all the cases.

EQs	P-Δ Effect	BF	DB	XB	CB	VB
E	P-Δ	2242.5	2157.4	730	299.3	139.4
	NPΔ	1569.7	577.4	569.9	245.43	119.9
K	P-Δ	1345.5	481.2	438.4	179.5	83.6
	NPΔ	941.8	336.9	306.9	125.7	58.5
L	P-Δ	1648.9	1255	1197.2	1096	1042.6
	NPΔ	1563.8	990.5	978.9	898.8	862
C	P-Δ	1502.5	1115.6	1002.6	802	664.9
	NPΔ	1051.7	803.2	782	657.6	571.86
N	P-Δ	1115.6	688.4	539	561.4	489.5
	NPΔ	780.9	495.6	460.3	420.4	421

*All the units are in MN-m, NPΔ- No P-Δ

(5) P-Δ Effect

Five different braced building systems were adapted in this research and five sets of strong earthquake motions were applied to each model where analyses were conducted considering with and without P-Δ effect. In case of both displacement and shear force, the magnitudes of shear force and displacement were increased in P-Δ analyses from without considering P-Δ effect. The percentage of increment of values of displacement and shear from without P-Δ to with P-Δ effects are depicted in the 8.

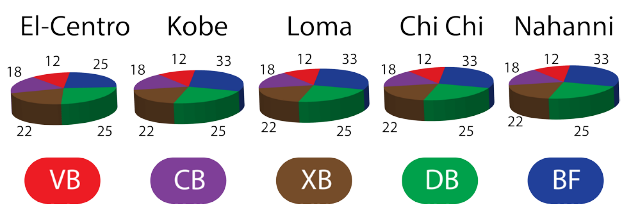

(a) Displacement

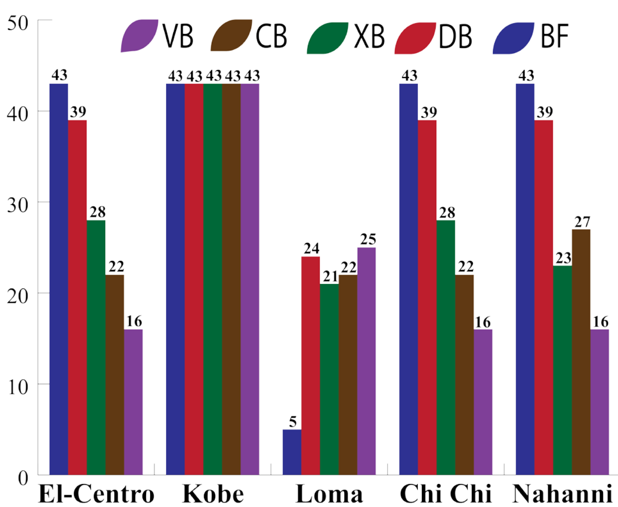

(b) Story shear

Figure 8. Percentage of increment of displacement and shear from without P-Δ to with P-Δ.

(6) Fragility curves

Fragility analysis is considered the most realistic probabilistic approach to observe the structural damage under different intensities of earthquakes. Incremental dynamic analysis (IDA) was performed for all the selected ground motions by varying their intensity from 0.1g to 1.4g. Five performance levels (OP, IO, DC, LS, and CP) stipulated by Xue et al. (2008) as presented in Table-7 were utilized to set the damage states and the following equation by Ibrahim & El-Shami (2011) was employed to obtain fragility curves for all the models.

$$P[D|PGA = \emptyset(\frac{\ln(PGA) - \mu}{\sigma})$$

** Φ= Standard normal cumulative distribution function

μ= Mean logarithmic peak ground acceleration (PGA)

σ= Standard deviation of logarithmic peak ground acceleration (PGA)

D= Damage state

Table 7. Overview of performance categories according to Xue et al. (2008)

Performance level	IDR (%)
Operational performance (OP)	0.5
Immediate occupancy (IO)	1.0
Damage control (DC)	1.5
Life safety (LS)	2.0
Collapse prevention (CP)	2.5

Fragility curves obtained from IDA and collapse fragility curves are illustrated in Figure-9 and 10, respectively. From the curves, it can be clearly seen that for ground motions with weak intensity (0.2g), no model has exceeded the probability of reaching Immediate Occupancy (IO) point apart from Model-1. Similar phenomena have been perceived for Damage Control (DC) point except Mdeol-1 which shows 96% possibility of structural damage.

However, all models exhibit 100% probability of crossing IO limit when subjected to ground motions with 1.0g or higher PGA. In case of Collapse prevention (CP) performance point, Model-1 illustrates the ultimate collapse of the structure and the possibility is maximum. All the other models equipped with various bracing systems presents very lower probability ranging from 4% to 10% and among them, Model-3 represents the lowest percentage, indicating its superior performance over other systems.

(5) Collapse Margin Ratio (CMR)

Proposed by FEMA (2010), Collapse margin ratio (CMR) is identified as one of the invaluable tools in the performance based seismic design of structures. CMR is often utilized to verify the results obtained from IDA. Table-6 represents the CMR values obtained from collapse fragility curves of all the models. FEMA (2010) proposes the following equation to compute the CMR of structures.

Collapse Margin Ratio, CMR= IC/IMCE

** IC= Maximum earthquake intensity from IDA curves

IMCE= Maximum capacity earthquake

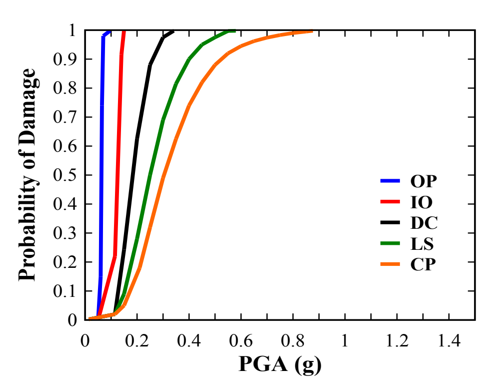

(a) Model-1

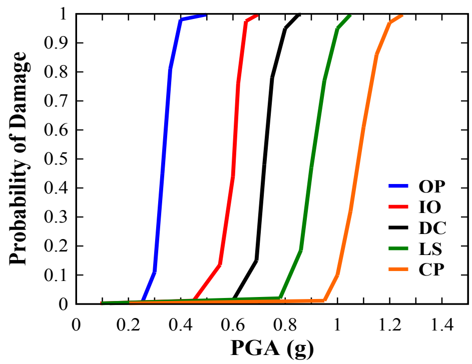

(b) Model-2

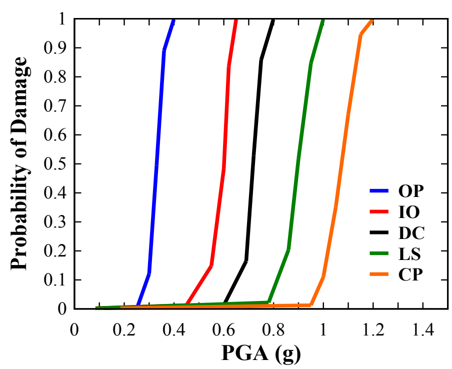

(c) Model-3

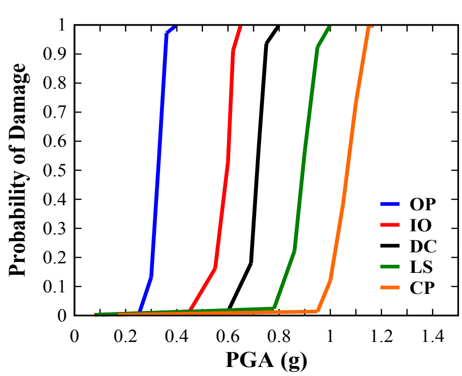

(d) Model-4

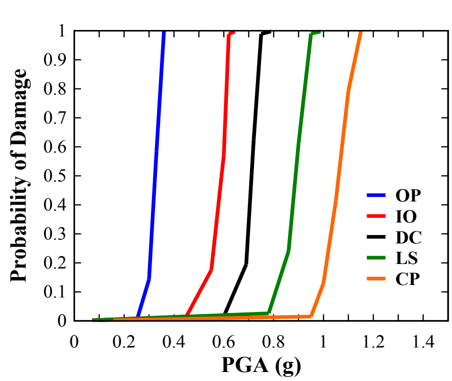

(e) Model-5

Figure 9. Fragility curves for all models

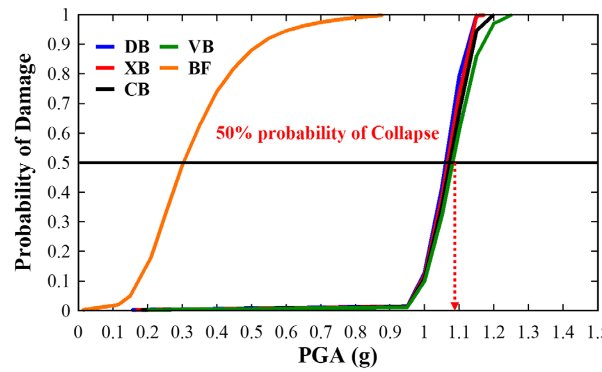

Figure 10. Collapse fragility curve of all models.

Table 8. Collapse margin ratio for all models

Model name	I_{MCE}(g)	I_C(g)	CMR= I_C/I_{MCE}
Model-1	0.25	0.31	1.24
Model-2	0.25	1.00	4
Model-3	0.25	1.09	4.36
Model-4	0.25	1.05	4.2
Model-5	0.25	1.02	4.08

From Figure-10, it is conspicuous that Model-3 (V braced frame) provides the highest seismic resistance and safety among the studied model building system as this model can withstand strong ground motions having PGA of more than 1. This evidence is also patent from Table-8 which shows the highest value of CMR for Model-3.

4. CONCLUSION

A g+30 storied building model is being utilized in this study to assess the retrofitting potential of different types of bracing systems based on NLTHA and IDA. From the observation of analysis results, the following decisions can be declared.

- The use of bracing systems for earthquake resistant structures significantly affected the base shear and displacement of the structure; these systems can be successfully used to increase the strength and rigidity properties against horizontal loads. VB systems are more efficient structures than other braced systems, because displacements and overturning moments of VB systems is lesser than the other braced systems. This can help the design engineers by indicating its superior performance during the selection of bracing system during the retrofitting of buildings.
- From the fragility curves, it can be seen that all the buildings retrofitted with various bracings (Model-2 to Model-5) are capable of withstanding the targeted MCE (0.25g) of the selected zone. Model-3 provides the best seismic strengthening.
- P-Δ effects increase the structural response twofold and hence it should be considered during the design phase of any tall structure. The BF structures are more vulnerable to P-Delta effect than the braced structures. The displacement

value for P-Δ analysis was increased from 12 to 33% for these studied bracing systems. Field engineers should be aware of verifying and cross-checking this criterion during the construction phase.

- For the seismic improvement of an existing structure, Model-3 is the most apropos choice in terms of resilience and safety.

REFERENCES

Avinash, T., & Pandian, G. A. M. (2017). Investigation of the effects of p-delta on tubular tall buildings. Technology, 8(2), 487-495.

Abbas, R. M., & Hassoni, A. N. (2018). Seismic Response of High Rise Steel Buildings Including Second-Order Effects. Association of Arab Universities *Journal of Engineering Sciences,* 25(1), 226-236.

Abdulkareem, A., & Abbas, R. (2020). Geometric nonlinear time domain spectral matching seismic analysis of base isolated high rise buildings including P-delta effect. *Journal of Engineering Science and Technology,* 15(5), 3104-3121.

American Society of Civil Engineers. (2017, June). Minimum design loads and associated criteria for buildings and other structures. American Society of Civil Engineers.

Chakraborty, S., Islam, M. R., & Kim, D. (2022). Structural Performance Assessment of Buildings Considering Beam Discontinuity and Horizontal Irregularity under Wind and Earthquake Loads. *Journal of the Korea Institute for Structural Maintenance and Inspection,* 26(5), 10-19. DOI: https://doi.org/10.11112/jksmi.2022.26.5.10

Carofilis Gallo, W. W., Clemett, N., Gabbianelli, G., O'Reilly, G., & Monteiro, R. (2022). Seismic resilience assessment in optimally integrated retrofitting of existing school buildings in Italy. Buildings, 12(6), 845. DOI: https://doi.org/10.3390/buildings12060845

Chakrawarty, M. (2022). Seismic Assessment of Structures Using P-Delta Effect (Doctoral Dissertation).

Cheng, H., Zhang, R., Zhang, T., Wang, H., Qu, C., & Zhang, P. (2022). P-Delta Effects on Nonlinear Seismic Behavior of Steel Moment-Resisting Frame Structures Subjected to Near-Fault and Far-Fault Ground Motions. Buildings, 12(2), 205. DOI: https://doi.org/10.3390/buildings12020205

Eskandari, R., Vafaei, D., Vafaei, J., & Shemshadian, M. E. (2017). Nonlinear static and dynamic behavior of reinforced concrete steel-braced frames. Earthquakes and Structures, 12(2), 191-200. DOI: https://doi.org/10.12989/eas.2017.12.2.191

Garg, A., & Sharma, A. (2020). Seismic Performance Evaluation Of A Multi-Storey Building With Different Braced Frames.

Goudar, S. S., & Talasadar, R. G. (2017). Buckling Analysis of RC Framed Structures with and Without Bracings. International Research Journal of Engineering and Technology, 4, 10.

Ibrahim, Y. E., & El-Shami, M. M. (2011). Seismic fragility curves for mid-rise reinforced concrete frames in Kingdom of Saudi Arabia. *The IES Journal Part A: Civil & Structural Engineering,* 4(4), 213-223.

Islam, M. R., Chakraborty, S., & Kim, D. (2022). Effects of Material Nonlinearity on Seismic Responses of Multistoried Buildings with Shear Walls and Bracing Systems. ARCHITECTURAL RESEARCH, 24(3), 75-84. DOI: https://doi.org/10.5659/AIKAR.2022.24.3.75

Islam, M. R., Chakraborty, S., & Kim, D. (2022). Effect of Plan Irregularity and Beam Discontinuity on Structural Performances of Buildings under Lateral Loadings. *ARCHITECTURAL RESEARCH,* 24(2), 53-61. DOI: https://doi.org/10.5659/AIKAR.2022.24.2.53

Islam, M. R., Chakraborty, S., Kong, B., & Kim, D. (2023). Seismic Fragility Analysis of Buildings with Combined Shear Wall-Damper System. *Journal of the Earthquake Engineering Society of Korea,* 27(2), 91-99. DOI: https://doi.org/10.5000/EESK.2023.27.2.091

Kircher, C., Deierlein, G., Hooper, J., Krawinkler, H., Mahin, S., Shing, B., & Wallace, J. (2010). Evaluation of the FEMA P-695 methodology for quantification of building seismic performance factors.

Khan, M. A., Varshney, M., & Nagar, B. (2019). Analysis of P-Delta Effect on High Rise Building.

Kumar, D. S. (2019). Analysis of High-rise Building for P-Delta Effect Using ETABS.

Lakshmanan, N. "Seismic evaluation and retrofitting of buildings and structures." *ISET Journal of earthquake technology,* 43, no. 1 (2006): 31-48.

Navya, G., & Agarwal, P. (2016). Seismic retrofitting of structures by steel bracings. Procedia Engineering, 144, 1364-1372. DOI: https://doi.org/10.1016/j.proeng.2016.05.166

Verma, R. K., & Singi, M. (2022). Comparative Study of High-Rise Building on Sloping Ground with Using Steel and RCC Bracing. Journal homepage: www. ijrpr. com ISSN, 2582, 7421.

Viji, A., Daniel, S., & Haamed, A. S. (2022). Seismic performance of RC frame retrofitted using steel bracing. Sustainability, Agri, Food and Environmental Research, 12. DOI: https://doi.org/10.7770/safer-V12N1-art2767

Xue, Q., Wu, C. W., Chen, C. C., & Chen, K. C. (2008). The draft code for performance-based seismic design of buildings in Taiwan. Engineering Structures. 30(6): 1535-1547. DOI: https://doi.org/10.1016/j.engstruct.2007.10.002

(Received Nov. 3, 2022/Revised Mar. 22, 2023/Accepted Mar. 28, 2023)